International Journal of Control and Automation
Vol. 8, No. 9 (2015), pp. 331-344
http://dx.doi.org/10.14257/ijca.2015.8.9.32

A Novel Direct Kinematic Method Based on Extended Kalman Filter for Stewart Platform

Rui Zeng[1], Yongjia Zhao[2] and Shulin Dai[3]

School of Automation Science and Electrical Engineering, BeiHang University
37 Xueyuan Road, Haidian District, Beijing, P.R.China[1,2,3]
shuihuoyanyan@163.com[1]; zhaoyongjia@buaa.edu.cn[2]; sldai@buaa.edu.cn[3]

Abstract

In this paper, the extended kalman filter based direct kinematic method was proposed to calculate the real-time end-effector position in a Stewart platform. A noise analysis based on the data transmission is proposed firstly, in which the size order of time domain noises is concerned. Then non-linear kinematic model and numerical method for Stewart platform are presented respectively. Later, an extended kalman filter based direct kinematic method is proposed, where transmission delays and synchronous errors are considered as a drift in the platform trajectory. Finally, various simulation results demonstrated the validity of the algorithm proposed in this article.

Keywords*: Stewart platform; Direct kinematic; Extended kalman filter*

1. Introduction

Direct kinematic problem is one of the most important issues in Stewart platform research, and both numerical and analytical methods have been used in this filed. Analytical methods, aim at a closed-form solution, relying on the configuration details of the mechanism and complex off-line calculation [1-4]. In real Stewart platform system, numerical direct kinematic methods are more widely used than analytical methods. When working on numerical methods, some researchers obtained the direct kinematic solutions by solving a high-order polynomial [5-8], while others were working on the non-linear kinematic equations [9, 12, 13].

Apart from classical Newton-Raphson algorithm, many new methods were employed in direct kinematic problem. Both Lim [10] and Ramesh [11] used neural network method to construct a non-linear mapping from actuator lengths to platform positions. Liu [12] combined immune algorithm, genetic algorithm and fuzzy theory to a hybrid system to solve direct kinematic problem. Wang [13] applied Lie algebra theory into Stewart platform kinematic analysis and then presented a simple direct kinematic method using small changes in joint variables. Eusebio et al. [14] chose the initial position value by probabilistic learning to avoid local minima of direct kinematic solutions.

To the best of authors' knowledge, the input values for direct kinematic method in all articles were assumed to be zero-noise signals. This indicates a need for data pretreatment function and a complex hierarchy in a real Stewart platform system [15].

The main idea in this paper is to present a one-step anti-noise direct kinematic method for real-time Stewart platform system, which means the algorithm will remove the noise itself during the direct kinematic procedure. The novel method is based on extended kalman filter (EKF),which have been proved to be useful in anti-noise system by numerous works [15-19].

The rest of this article is organized as follows. Basic ideas and theories for real-time Stewart platform system are reviewed in section two. In section three, system

ISSN: 2005-4297 IJCA

noise analysis and Extended kalman filter based direct kinematic (EBDK) method are presented. In section four, numerical simulations are performed to validate the EBDK method. Conclusions are made in section five.

2. Stewart Platform System Overview

A real-time control system for Stewart platform used in flight simulator is shown in Figure 1. The definition of "real-time" is different between hierarchies.

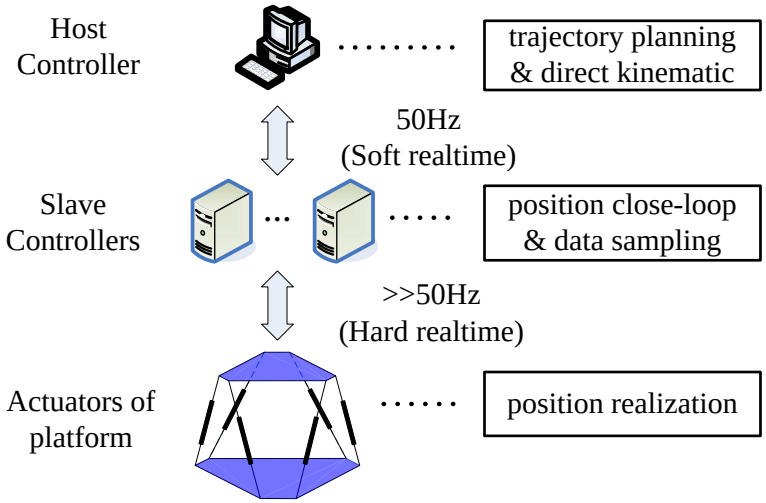

Figure 1. Real-time Stewart Platform System

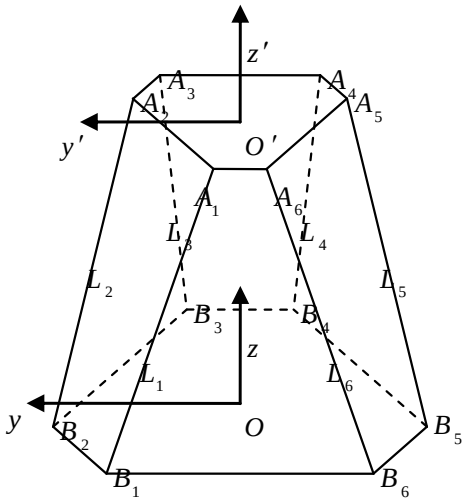

Figure 2. Stewart-Gough Platform

A real Stewart platform system considers not only the direct kinematic algorithm but also the data transmission procedure. We introduce them respectively in this section.

2.1. Kinematic for Stewart Platform

Commonly, six-dimensional vector P indicates the position and orientation of the end-effector in $Oxyz$ coordinate frame, and six-dimensional vector l indicates the actuators' lengths. Then under the right-hand coordinate system $Oxyz$ defined in Figure 2, the reverse kinematic model of Stewart platform can be presented as follows [1].

$$l_i = \left\| P_{o'} + A_i - B_i \right\| = \left\| P_{o'} + RA_i' - B_i \right\| \quad (1)$$

where l_i is the length for i'th actuator

$P_{o'}$ is the coordinate of $\underline{O'}$ in $Oxyz$ frame

A_i B_i are the values of OB_i and $O'A_i$ in $Oxyz$ frame

A_i' is the value of $O'A_i$ in $O'xyz$ frame

R is the transform matrix from $O'xyz$ frame to $Oxyz$ frame

The velocity kinematic equation is the derivative of equation (1). Assuming $J(P)$ is the Jacobi matrix in position P, the velocity kinematic is given as.

$$\dot{l} = J(P) \cdot \dot{P} \quad (2)$$

We assume all Stewart mentioned in this article can be expressed by equation (1) and (2).

2.2. Direct Kinematic Algorithm

A direct kinematic problem for Stewart platform is to find the unknown end-effector position based on actuator lengths with constraints in equation (1). The common numerical direct kinematic method is given as follow.

1)Choose the initial position for P in a proper domain based on known actuator lengths l or experience;

2)Set the condition coefficient ε_c for the iterated result accuracy, set the penalty coefficient ε_p for position correction.

3)Calculate a position correction ΔP based on multiple algorithms.

4)If $\left\| f_p(P, \Delta P) \right\|_* \le \varepsilon_p$,then $P = P + \Delta P$; else, back to 3 for a new ΔP .

5)If $\left\| f_c(P, l) \right\|_* \le \varepsilon_c$, then output the present P as the result; else ,back to 3 for a new iteration.

$\| \|_*$ denotes norms in corresponding generalized space. Mainly, step 1 decides the applicability of the algorithm, Step 3 to 5 relate to the convergence rate, algorithm robustness and result accuracy respectively.

2.3. Data Transmission and Time Synchronization

In this work, the soft real-time transmission is based on an Ethernet protocol (IEEE 802.3u conformed). We use a NTP time-synchronously method to estimate the time and frequency offsets between host and slaves [20]. The synchronization equation is given as follows.

$$T = X_i t_i + Y_i \quad (3)$$

where T is the time in host controller; t_i is the time in i'th slave controller; X_i is the frequency ratio between host clock and i'th slave clock ; Y_i is the time offset of slave clock to host clock

A typical real-time direct kinematic procedure for Stewart platform is shown in Figure 3, and we ignore all possible noises here. In time t^0, the slave controllers send host all the N sample signals in the previous transmission interval(denoted by

T_s). After direct kinematic and time rectification, trajectory points in time T^0 are obtained. The interpolation estimates the real trajectory in host controller finally. In both Figure 3 and Figure 4, the horizontal axis represents the time, and norm values for P or l are recorded on vertical scale.

3. EKF Based Direct Kinematic Procedure

According to the background knowledge in the last section, module based noise analysis and common numerical direct kinematic algorithm are presented here respectively. Then EBDK procedure will be introduced .

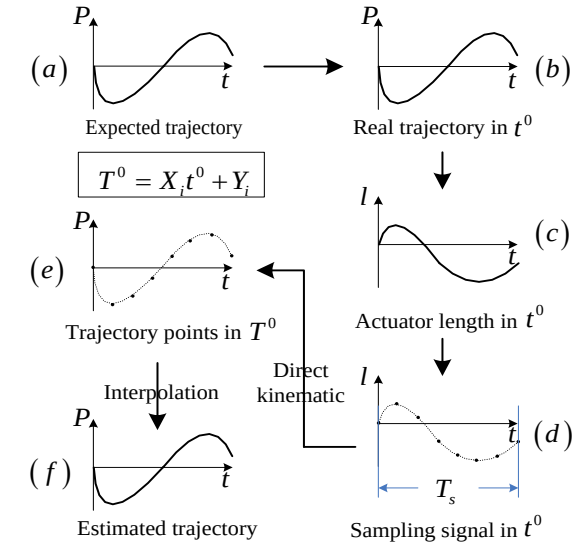

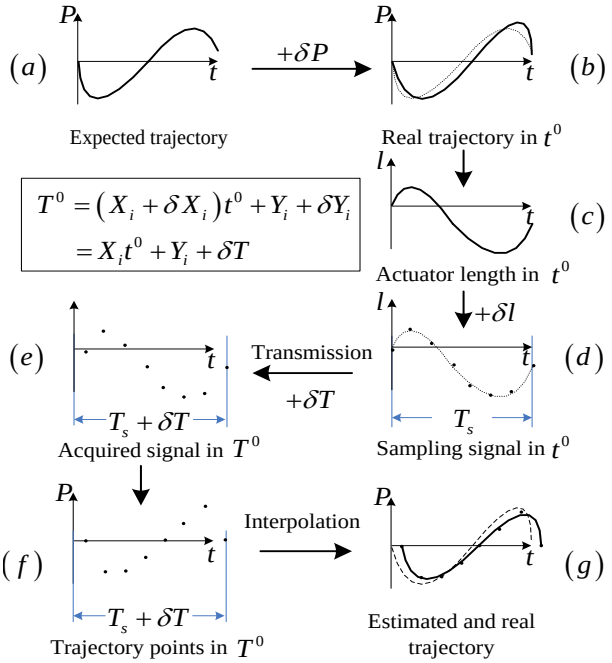

Figure 3. Data Transmission Procedure-I Figure 4. Data Transmission Procedure-II

3.1. Noise Analysis

Measurement errors and transmission deviation are two main data noise sources. The noise caused by time synchronization drift in distributed network situation is studied by many researchers [18,19].

A complete real-time direct kinematic procedure in one sampling period T_s for Stewart platform is shown in Figure 4. Expected trajectory is realized under realization noise δP (a,b), and the slave controllers get a group of actuator length based sampling signals with sampling noise δl (c,d). Then the uncertain transmission delay affects the direct kinematic results by transmission noise δT (e,f). Finally, both the estimated trajectory(solid) and real trajectory(dashes) are shown in (g).

Based on equation (3), the synchronization equation with noise is given as follows.

$$\begin{aligned} T &= (X_i + \delta X_i) t_i + Y_i + \delta Y_i \\ &= X_i t_i + Y_i + \delta T_i \end{aligned} \tag{4}$$

where δX_i is the frequency rate drift between host clock and i'th slave clock during the transmission period; δY_i is the time offset drift between i'th slave clock and host clock during the transmission period; δT_i is the transmission noise for i'th slave controller.

Assume that δX_i is the same during the transmission period. And in the linear system (4), δT_i can be rewritten as follows.

$$\delta T_i = \delta X_i \cdot t_i + \delta Y_i = \delta X_i \cdot T_s + \delta Y_i \tag{5}$$

Commonly, all six δX_i and δY_i are assumed to be a normal distribution[18], then $\{\delta T_i\}_{i=1\cdots 6}$ is a group of orthogonal Gaussian noise with same statistic characteristics. Under harsh network situation, the δY_i satisfies a truncated normal distribution limited by Y_i. The statistic characteristics for $\{\delta T_i\}_{i=1\cdots 6}$ are shown as follows.

General situation:

$$E(\delta T_i) = 0 \quad Var(\delta T_i) = T_s \cdot \sigma_{X_i}^2 + \sigma_{Y_i}^2 \tag{6-1}$$

Harsh network situation:

$$E(\delta T_i) = \frac{\phi\left(-T_s/\sigma_{Y_i}\right)}{1 - \Phi\left(-T_s/\sigma_{Y_i}\right)} \sigma_{Y_i} \tag{6-2a}$$

$$\begin{aligned} Var(\delta T_i) &= T_s \cdot \sigma_{X_i}^2 + \\ &\sigma_{Y_i}^2 \left[1 + \frac{-T_s/\sigma_{Y_i}\, \phi\left(-T_s/\sigma_{Y_i}\right)}{1 - \Phi\left(-T_s/\sigma_{Y_i}\right)} - \left(\frac{\phi\left(-T_s/\sigma_{Y_i}\right)}{1 - \Phi\left(-T_s/\sigma_{Y_i}\right)} \right)^2 \right] \end{aligned} \tag{6-2b}$$

We also assume both the realization noise δP and sampling noise δl are Gaussian noises in this paper.

3.2. EKF in Direct Kinematic

Extended kalman filter is designed especially for weak nonlinear system. Then the state update function and observation function for Stewart system are shown as follows.

$$\begin{cases} P_k = P_{k-1} + \Delta t_i \cdot \dot{P}_{k-1} + W_k \\ l_k = f(P_k) + V_k \end{cases} \tag{7}$$

where P_k is the estimated end-effector position at time k ; Δt_i is the interval between two sampling data; $\dot{P}_{k-1}$ is the end-effector position in $k-1$ time; W_k is the process update noise in k time; l_k is the sampled actuator length in k time; $f(\cdot)$ is the inverse kinematic shown in (1); V_k is the observation noise in k time

According to the design principle in [16] and equations(1,2,5,6), we have the EKF equations for the direct kinematic method given as follows.

Priori estimation at time k based on the previous step position state, covariance matrix and kalman gain are given as

$$\hat{P}_{k|k-1} = \hat{P}_{k-1} + \Delta t_i \cdot \dot{P}_{k-1} \tag{8-1}$$

$$U_{k|k-1} = U_{k-1} + Q_k \tag{8-2}$$

$$K_k = U_{k|k-1} \cdot H_k^T \cdot \left(H_k \cdot U_{k|k-1} \cdot H_k^T + R_k \right)^{-1} \tag{8-3}$$

Posterior estimation for position state and covariance are given as

$$\hat{P}_k = \hat{P}_{k|k-1} + K_k \cdot \left(l_k - f\left(\hat{P}_{k|k-1} \right) - E\left(V_k \right) \right) \tag{8-4}$$

$$U_k = (I - K_k \cdot H_k) U_{k|k-1} \tag{8-5}$$

Here we define H_k to be the Jacobi matrix in position $\hat{P}_{k|k-1}$.

$$H_k = \left. \frac{\partial l}{\partial P} \right|_{\hat{P}_{k|k-1}} = J\left(\hat{P}_{k|k-1} \right) \tag{9-1}$$

As shown in Figure 4, the real trajectory equals to an expected trajectory with noise δP , which means

$$W_k = \delta P \tag{9-2}$$

Then we use expected speeds instead of the outputs of speed sensors here, and covariance matrix Q_k is based on δP . Since the transmission noise δT lead to a offset of l , the observation noise satisfies the following equation,

$$V_k = \delta T * \dot{l} + \delta l \tag{9-3}$$

Then covariance matrix R_k is based on δT and δl .

Because of the existence of noise, the EBDK algorithm eliminates an accuracy verification step. Then an EBDK (EKF based real-time direct kinematic) method can be given as follows.

1)Choose previous estimated result P^0 or an empirical value to be the initial position for P ; Set the penalty coefficient ε for step maximum;

2)Arrange the sampling date in one transmission period T_s as $\left(l^1, \cdots, l^N \right)$;

3)Estimate the position P^i based on l^i using the EKF equations given in (8).

4)If $\left\| f_p\left(P^{i-1}, P^i \right) \right\|_* > \varepsilon$, then $P^i = P^{i-1}$, $\Delta t_i = \Delta t_i + \Delta t_{i-1}$ and mark the l^i ;

5)Output P^i ; if $i < N$, back to step 3);

6)List marked l^i and back to step 1) for a new iteration.

4. Simulation and Analysis

The coordinates for all the terminal points of Stewart platform are shown in Figure 2 and table 1.

Table 1. The Coordinates for Terminals

Actuators	End-effector Terminals	BaseTerminals
l_1	A_1 (-1.9544,0.0481,3)	B_1 (-1.4269,2.3695,0)
l_2	A_2 (0.9355,1.7166,3)	B_2 (-1.3386,2.4205,0)
l_3	A_3 (1.0189,1.6685,3)	B_3 (2.7655, 0.051, 0)
l_4	A_4 (1.0189,-1.6685,3)	B_4 (2.7655, -0.051,0)
l_5	A_5 (0.9355,-1.7166,3)	B_5 (-1.3386,-2.4205,0)
l_6	A_6 (-1.9544,-0.0481,3)	B_6 (-1.4269,-2.3695,0)

Because of the difference between displacement and rotation in $SE(3)$ space, we define a new norm shown in (10) to measure the "distance" between two position instead of the 2-norm.

$$\left\| P^0, P^1 \right\|_* = \left\| A_1^0, A_1^1 \right\|_2 + \left\| A_2^0, A_2^1 \right\|_2 \cdots + \left\| A_6^0, A_6^1 \right\|_2 \tag{10}$$

where $\left\| A_1^0, A_1^1 \right\|_2 = \sqrt{\left(A_{1x}^0 - A_{1x}^1 \right)^2 + \left(A_{1y}^0 - A_{1y}^1 \right)^2 + \left(A_{1z}^0 - A_{1z}^1 \right)^2}$

We expect the end-effector to move along a trajectory o given in (11), notice that $P = \left(P_x, P_y, P_z, P_\alpha, P_\beta, P_\gamma \right)$.

$$o\big|_t \rightarrow \begin{cases} P_x = 2.5\sin\left(\omega t\right) \\ P_y = 2.5\sin\left(\omega t + \pi/6\right) \\ P_z = \sin\left(\omega t + \pi/3\right) + 3 \\ \dot{P}_\alpha = 0.16\pi\sin\left(\omega t + \pi/2\right) \\ \dot{P}_\beta = 0.16\pi\sin\left(\omega t + 2\pi/3\right) \\ \dot{P}_\gamma = 0.16\pi\sin\left(\omega t + 5\pi/6\right) \end{cases} \tag{11}$$

4.1. Validity and Verification

In simulation, we consider three noise situations for a real Stewart platform system. All default parameters are shown in table 2 in which $\sigma_p = 0.0005C_i$ (C_i correspond to the displacement maximum of the end-effector in the six axis of $SE(3)$ space). σ_Y is denoted as "Sigma" in all figures.

Table 2. Variables for Simulation-I

Variable	Value	Noise	Description
ω	1	δP_i	$N\left(0, \sigma_p^2\right)$
T_s	0.02	δX_i	$N(0,(10^{-5})^2)$
X_i	1	δY_i^1	$N(0,(0.006)^2)$
Y_i	0.001	δY_i^2	$N(0,(0.003)^2)$
N	1	δY_i^3	$N(0,(0.001)^2)$

We assume δY_i to be a normal distribution firstly, and test the EKF based direct kinematic method under three kinds of δY_i. Newton-Raphson method [21] is used for comparison purpose. The inputs of Newton method is the sampling data after time synchronization. The simulation results for three kinds of δB_i are shown in Figure 5 and Figure 6.

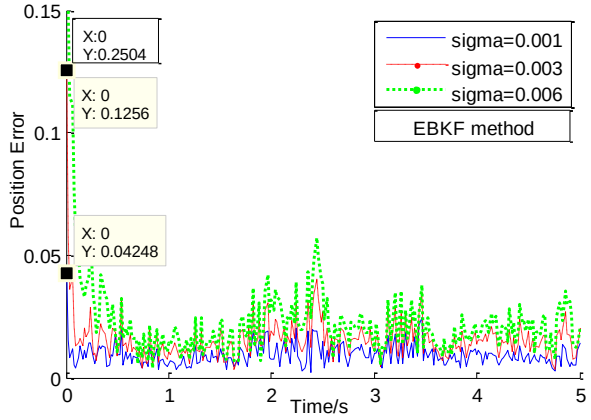

Figure 5. Position Error for EBDK Method

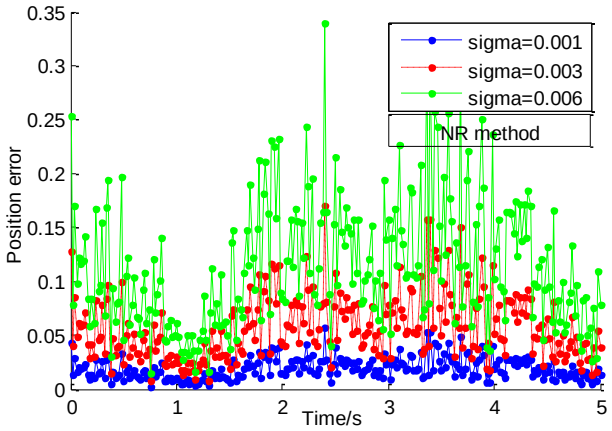

Figure 6. Position Error for NR Method

Compared to the NR method, it's clearly that the EBDK method is effective in removing most noise in all three situation.

In Figure 5 and Figure 6, the residual noises in position errors are in direct proportion to σ_Y in both two methods. This conclusion is also demonstrated in Figure 7. As we claimed in previous section, the δY_i will satisfy a truncated normal distribution under special network condition. After appropriate organization, the simulation results of EBDK method under both normal and half-normal distribution(a typical truncated normal distribution) noise are shown in Figure 7. The vertical axis presents the mean value of position error under a five second simulation.

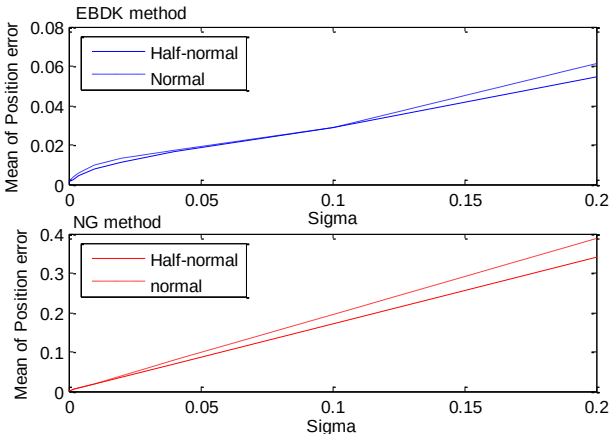

Figure 7. Different Distribution Noises

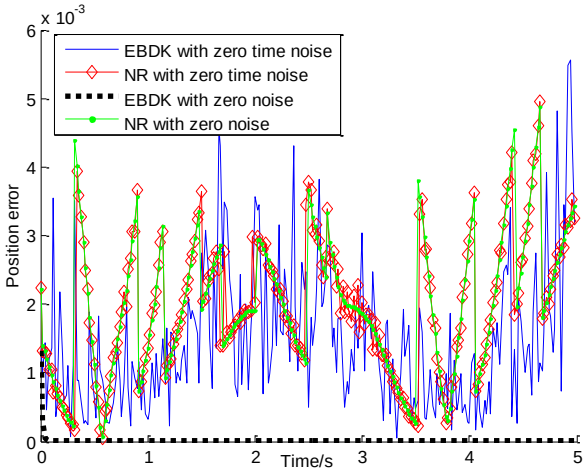

Figure 8. Zero-noise Responses

With same σ_Y, the differences between the dashes and solids are affected by the statistic characteristics shown in (6). And the change trends are almost the same for two lines. In later experiments, we only discuss the normal distribution situation.

Based on the kalman filter theory, the EBDK method is also effective in zero-noise situation. Two zero-noise simulations are conducted to verify the algorithm's effectiveness. Shown as in Figure 8, EBDK method has a zero-error output in zero-noise situation and a limited-error output in zero-time-noise situation. The NR method which relied on the condition coefficient ε_c fails to defend residual errors in both zero noise situations.

4.2. Simulative Experiments

Numerous simulations are conducted to verify the effects of ω and N in the EBDK method. The default parameters for the simulation are listed in table 3. Statistical analysis of the simulation results is performed to draw clear conclusions.

Table 3. Variables for Simulation-II

Variable	Value	Noise	Value
T_s	$0.02s$	δP_i	$(0, 0.0005C_i)$
X_i	1	δX_i	$(0, 10^{-5})$
Y_i	0.001		

According to (5), the $\dot{l}$ plays an key role in V_k, then ω effects V_k through $\dot{l}$. We test the mean of position error for both methods under different ω. Simulation results with respected to different δY_i are shown in Figure 8 and Figure 9.

Statistic results in Figure 9 demonstrate that the ω plays a positive role in the output position errors. From Figure 10, the EBDK method has a worse performance than NR method in a small ω situation. Notice the existence of maladjusted data in NR method(in Figure 9). It's a typical calculation mistake when choosing an unsuitable ε_p.

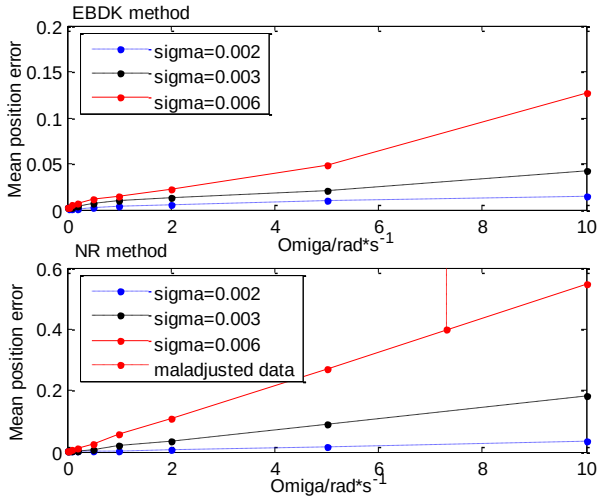

Figure 9. Affection of ω in Simulation

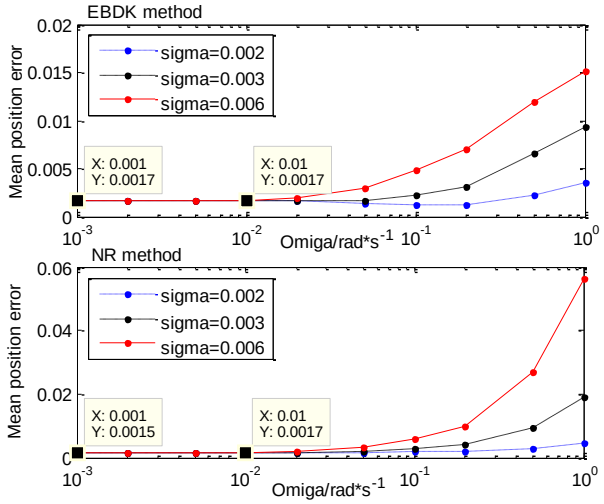

Figure 10. Details for the Affection of ω

In real system, the sampling rate is higher than the transmission rate, thus the direct kinematic module acquire a group of sampling data once. Figure 11 is the position error change during a four seconds simulation with different sampling rate, in which $\sigma_\gamma = 0.003$. Notice the sampling rate is N times of transmission rate.

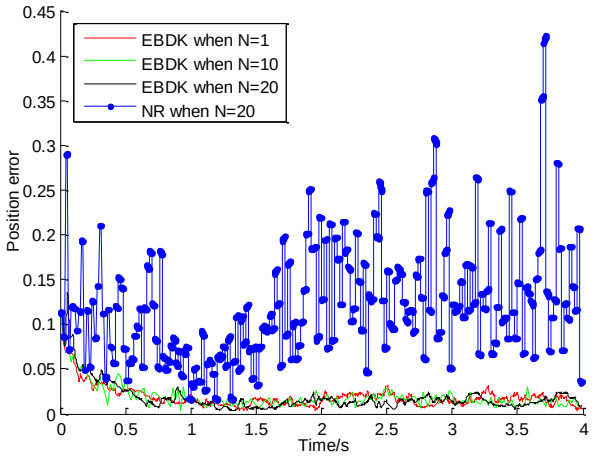

Figure 11. Affection of Sampling Rate-I

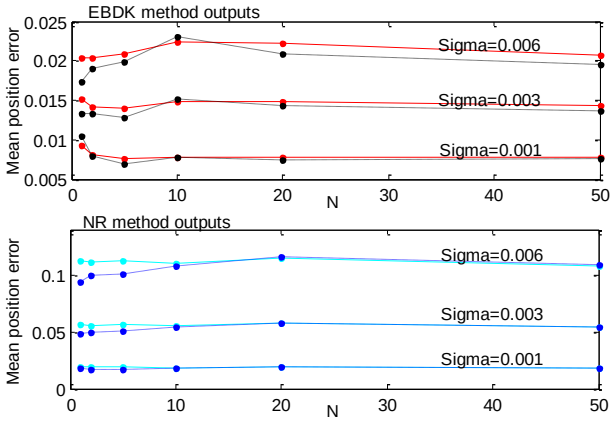

Figure 12. Affection of Sampling Rate-II

The output position errors of EBDK method under three sampling rates are in a same level in Figure 11. This indicate the sampling rate don't affect the estimation accuracy of EBDK. And the statistic characteristics for the simulations shown in Figure 12 also support this conclusion.

The density of sampling points do affects the estimation accuracy for random points in the trajectory. We choose one hundred rand points in time domain and estimate the respective position by interpolation firstly. The interpolation is based on the outputs of EBDK method and NR method respectively. Then we calculate the position errors of these respective positions later. The mean of position errors for rand points are compare to the mean of output position errors of two direct kinematic methods finally. The simulation results are shown in Figure 12, in which solid lines represent direct kinematic algorithm outputs and dash lines represent random points.

With different noise, the mean of position errors for both rand points and sampling points have the same change trend as shown in Figure 10. And the average difference between rand points and sampling points converge when the sampling

rate increase. Base on the simulation results, we can draw a conclusion that redundant sampling data are not always indispensable for a real-time system when using either EBDK method or NR method.

5. Conclusion

To avoid the noises during the data sampling and transmission process, we develop an EBDK algorithm for real-time Stewart platform system. The simulation results demonstrate that this method is effective for noise rejection purpose in most simulation environment.

Acknowledgement

Zeng Rui thanks for the suggestions and help from Dr. Qingya Wu, Dr. Dongdong Zheng and Dr. lijun Li.

References

[1] C. Innocenti, "Forward kinematics in polynomial form of the general Stewart platform", Journal of Mechanical Design, vol.123, no.2, **(2001)**, pp.254-260.
[2] P. Ji and H. T. Wu, "A closed-form forward kinematics solution for the 6-6p Stewart platform", IEEE Transactions on Robotics and Automation, vol.17, no.4, **(2001)**, pp.522-526.
[3] I. A. Bonev, "Geometric analysis of parallel mechanisms", PhD diss., University Laval, **(2002)**.
[4] X. S. Gao, D. Lei and G. F. Zhang, "Generalized Stewart-Gough platforms and their direct kinematics", IEEE Transactions on Robotics, vol.21, no.2, **(2005)**, pp.141-151.
[5] N. Prabjot, K. J. Waldron and V. Murthy, "Direct kinematic solution of a Stewart platform", IEEE Transactions on Robotics and Automation, vol.6, no.4, **(1990)**, pp.438-444.
[6] M. Raghavan, "The Stewart platform of general geometry has 40 conFigure urations", Journal of Mechanical Design, vol.115, no.2, **(1993)**, pp.277-282.
[7] S. M. Song, "Forward position analysis of nearly general Stewart platforms", Journal of Mechanical Design, vol.116, no.1, **(1994)**, pp.54-60.
[8] I. D. Akcali and H. Mutlu, "A novel approach in the direct kinematics of Stewart platform mechanisms with planar platforms", Journal of Mechanical Design, vol.128, no.1, **(2006)**, pp.252-263.
[9] J. P. Merlet, "Solving the forward kinematics of a Gough-type parallel manipulator with interval analysis", The International Journal of robotics research, vol.23, no.3, **(2004)**, pp.221-235.
[10] K. B. Lim, "Forward kinematics solution of Stewart platform using neural networks", Neurocomputing, vol.16, no.4, **(1997)**, pp.333-349.
[11] P. R. Kumar and B. Bandyopadhyay, "The forward kinematic modeling of a Stewart platform using NLARX model with wavelet network", Industrial Informatics (INDIN), 11th IEEE International Conference, IEEE, **(2013)**; Bochum,Germany.
[12] L. Sheng, L. Wanlong, D. Yanchun and F. Liang, "Forward kinematics of the Stewart platform using hybrid immune genetic algorithm", Mechatronics and Automation, Proceedings of the IEEE International Conference, IEEE, **(2006)**; Luoyang,China.
[13] Y. F. Wang, "A direct numerical solution to forward kinematics of general Stewart–Gough platforms", Robotica, vol.25, no.1, **(2007)**, pp.121-128.
[14] E. Martinez, E. Hernández, S. I. V. Peña and E. S. Soto, "Towards a Robust Solution of the Non-linear Kinematics for the General Stewart Platform with Estimation of Distribution Algorithms", Int J Adv Robotic Sy, vol.10, no.38, **(2013)**.
[15] Q. Li, H. Zhang, P. Q. Ye and G. H. Duan, "6 DOF long-range precision tracking system", Systems, Man and Cybernetics, IEEE International Conference, IEEE, **(2004)**.
[16] S. S. Haykin, ed. "Kalman filtering and neural networks", New York: Wiley, **(2001)**.
[17] D. Theodorakatos, E. Stump and V. Kumar, "Kinematics and pose estimation for cable actuated parallel manipulators", ASME International Design Engineering Technical Conferences and Computers and Information in Engineering Conference, American Society of Mechanical Engineers, **(2007)**; Las Vegas, U.S.A.
[18] J. Tang, H. S. Shi, R. H. Hou and X. S. Li, "Time synchronization algorithm in sensor network based on kalman filter", Communication Technology, ICCT, International Conference, IEEE, **(2006)**; Guilin, China.
[19] Y. Sun and J. Y. Hao, "Adaptive timing synchronization based on extended Kalman filter for Wavelet Packet Modulated signals", Wireless Communications & Signal Processing, WCSP, International Conference, IEEE, **(2009)**; Nanjing, China.

[20] D. L. Mills, "Internet time synchronization: the network time protocol", Communications, IEEE Transactions, vol.39, no.10, **(1991)**, pp.1482-1493.
[21] P. R. McAree and R. W. Daniel, "A fast, robust solution to the Stewart platform forward kinematics", Journal of robotic systems, vol.13, no.7, **(1996)**, pp.407-427.

Authors

Rui Zeng, he received his B.E. degree in Automation Science from Beijing Information Science and Technology University, China, in 2008, and his M.E degree in Automation Science from Beihang University, China, in 2011. He is currently a Ph.d candidate in Automation Science and Electrical Engineering School of Beihang University. His research interests include parallel robot application and visual servo.

Yongjia Zhao, he received the B.E. degree in Aircraft Design and Applied Mechanics and Dr. Eng. degree in Navigation, Guidance and Control from Beihang University, China, in 2002 and 2010 respectively. He is currently a lecturer at the School of Automation Science and Electrical Engineering, Beihang University. His research interests include flight simulation and computer vision.

Shuling Dai, he received the B.E. degree in Automation Science, M.E. degree in Robot Control and Dr. Eng. degree in Navigation, Guidance and Control from Beihang University, China, in 1988, 1991 and 1997 respectively. He is currently a professor at School of Automation Science and Electrical Engineering, Beihang University. His research interests include virtual reality, flight simulation and distributed computing. He is Deputy Director of China State Key Lab of Virtual Reality.